

Realisation of nonreciprocal transmission and absorption using wave-based active noise control ^{EP}

Cite as: JASA Express Lett. 2, 054801 (2022); <https://doi.org/10.1121/10.0010454>

Submitted: 09 January 2022 • Accepted: 19 April 2022 • Published Online: 10 May 2022

 Joe Tan,  Jordan Cheer and Steve Daley

COLLECTIONS

 This paper was selected as an Editor's Pick



ARTICLES YOU MAY BE INTERESTED IN

Machine learning in acoustics: Theory and applications

The Journal of the Acoustical Society of America **146**, 3590 (2019); <https://doi.org/10.1121/1.5133944>

Secondary channel estimation in spatial active noise control systems using a single moving higher order microphone

The Journal of the Acoustical Society of America **151**, 1922 (2022); <https://doi.org/10.1121/10.0009837>

Waveguide invariant in a gradual range- and azimuth-varying waveguide

JASA Express Letters **2**, 056002 (2022); <https://doi.org/10.1121/10.0010489>


Read Now!

JASA
THE JOURNAL OF THE
ACOUSTICAL SOCIETY OF AMERICA

Special Issue:
Lung Ultrasound



Realisation of nonreciprocal transmission and absorption using wave-based active noise control

Joe Tan,^{a)}  Jordan Cheer,  and Steve Daley

University of Southampton, Southampton, Hampshire, SO17 1BJ, United Kingdom

j.tan@soton.ac.uk, j.cheer@soton.ac.uk, s.daley@soton.ac.uk

Abstract: Nonreciprocal acoustic devices typically break reciprocity by introducing nonlinearities or directional biasing. However, these devices are generally not fully adaptable and often use resonant cavities, which only exhibit nonreciprocal behaviour over a narrow bandwidth. Therefore, to overcome these challenges, this paper investigates how wave-based active control can be used to achieve broadband nonreciprocal behaviour in a one-dimensional environment. Wave-based controller architectures are described for both transmission and absorption control and, through simulation and experimental implementations, it is shown that they can achieve broadband nonreciprocal behaviour. Importantly, the direction of nonreciprocal behaviour can be straightforwardly reversed. © 2022 Author(s). All article content, except where otherwise noted, is licensed under a Creative Commons Attribution (CC BY) license (<http://creativecommons.org/licenses/by/4.0/>).

[Editor: Charles C. Church]

<https://doi.org/10.1121/10.0010454>

Received: 9 January 2022 **Accepted:** 19 April 2022 **Published Online:** 10 May 2022

1. Introduction

Reciprocity is a fundamental acoustic property that describes the symmetry of sound transmission between two points, which has been utilised in many acoustic applications to simplify acoustic measurement processes.^{1,2} However, reciprocity is undesirable in certain applications and this has led to significant interest in the development of nonreciprocal acoustic devices. These devices allow acoustic waves to propagate unimpeded in one direction, whilst blocking the acoustic waves propagating in the opposite direction. Typically, the symmetry of transmission has been broken by introducing nonlinearities,^{3–7} fluid motion,⁸ or spatiotemporal modulation of resonant cavities.^{9–11} These various approaches have different limitations, which include the following: nonlinear nonreciprocal devices can introduce unwanted harmonic components; additional flow noise is added into the system when fluid motion is used to realise nonreciprocal behaviour; the bandwidth over which nonreciprocal behaviour is realised is narrow when relying on the properties of resonant cavities; and, finally, many of these systems are not easily adaptable to allow the direction of nonreciprocal behaviour to be reversed. Some of these issues have recently been overcome through the realisation of a non-local active metamaterial consisting of an array of sensor-actuator pairs, which can create the directional biasing required to achieve broadband nonreciprocal sound transmission.^{12,13} However, this broadband linear nonreciprocal device is not fully adaptable because the sensor-actuator arrangement creates a preferential direction for the nonreciprocal behaviour. In addition, nonreciprocal absorption has not yet been realised in the acoustic domain, although it has been observed in the electromagnetic domain.^{14,15} Therefore, this paper investigates how active control can be used to control the transmitted and reflected wave components to achieve broadband nonreciprocal sound transmission and absorption in a one-dimensional linear system and proposes a system setup that allows the direction of nonreciprocal behaviour to be easily reversed. Two different active control strategies have been used in this paper: in the first case, a single monopole control source is driven to minimise the transmitted wave; in the second case, a pair of monopole control sources are driven to minimise the transmitted and reflected wave components. The performance of the proposed wave-based active controllers was first investigated in the theoretically modelled case, which assumes an infinite duct and acoustic point sources, before being implemented experimentally using finite-sized practical loudspeakers to realise the acoustic sources and a real-time controller.

2. System description

The physical configuration of the proposed active control system for the realisation of both nonreciprocal transmission and absorption control in a one-dimensional duct system is presented in Fig. 1. In both the theoretical and experimental cases, the system consists of an impedance tube with an anechoic termination and primary source at each end, and an active control unit placed at the centre of the duct with two pressure sensors located either side of the unit. The active control unit consists of the control source and the wave-based active controller, which adaptively filters the signal

^{a)} Author to whom correspondence should be addressed.

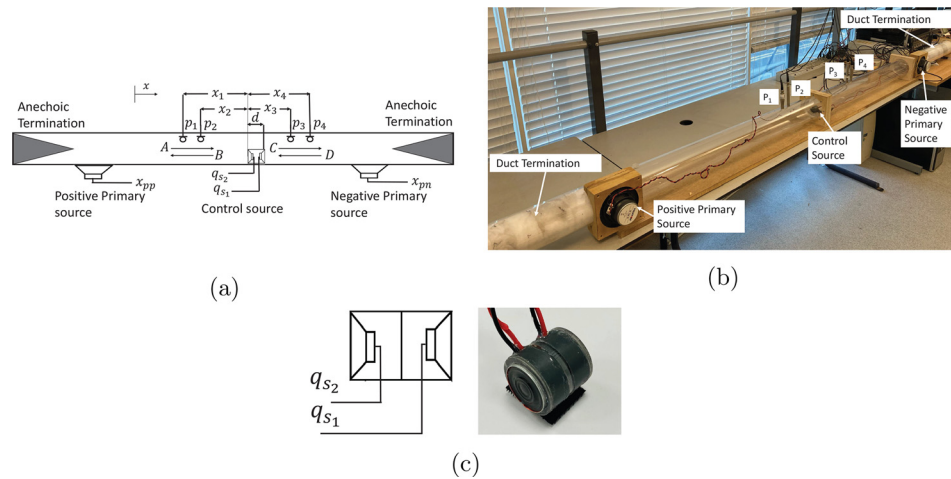


Fig. 1. The theoretical (a) and experimental (b) configurations of the proposed active nonreciprocal sound transmission and absorption control systems for a one-dimensional acoustic system. (c) The pair of monopole control sources used in this paper for the experimental validation.

measured by each sensor to drive the control sources to achieve the desired wave manipulation. The positive and negative propagating wave components, with coefficients A to D , are also shown in Fig. 1(a). When the incident sound field is generated by the positive primary source shown in Fig. 1(a), the positive propagating upstream wave, A , is the incident wave, C is the positive propagating transmitted wave component, whilst B and D are the negative propagating upstream and downstream reflected wave components. However, when the incident sound field is generated by the negative primary source, the negative propagating downstream wave, D , is the incident wave, B is the negative propagating transmitted wave, whilst C and A are now the positive propagating upstream and downstream reflected wave components, respectively. Throughout this paper, the subscripts $+$ and $-$ show the corresponding wave components generated by either a positive or negative primary source, respectively. To control the transmitted and reflected wave components individually, they need to be separated from the total pressure measured at each of the sensors and this has been carried out via the integration wave separation method proposed by Zhu *et al.*¹⁶ This wave separation method has been chosen because the incident and reflected wave components are completely separated, which means that the incident wave can be used as the reference signal for broadband feedforward control.¹⁶

The system shown in Fig. 1(a) is consistent for both the theoretical simulations that will be presented in Sec. 3.1 and the experimental implementation presented in Fig. 1(b), which will be described in Sec. 3.2. The system parameters that are used in both cases are detailed in Table 1. Based on these system parameters, the upper frequency limit of 1.6 kHz has been imposed so that the duct diameter is larger than the shortest considered acoustic wavelength and only plane waves propagate in the duct. The low frequency limit is imposed by the assumption upon which the integration wave separation method is based. Specifically, it is assumed that evanescent wave components produced by the control sources are negligible and, therefore, a pair of microphones can be used to separate the positive and negative propagating wave components. This assumption requires that the pressure sensors are located at a sufficient distance from the control sources such that the near-field contribution from the control sources has decayed to a level that is negligible in comparison to the propagating components. Based on previous work,^{17,18} it is assumed that the evanescent waves can be neglected provided that they have decayed to 10% of their original values and, given the shortest distance between the sensors and control sources presented in Table 1, this condition is met for frequencies greater than 560 Hz, which defines the lower frequency limit for this system. This limit is only relevant to the experimental setup, since the near-field of the control sources has not been modelled in the theoretical case.

2.1 Wave-based active control formulations

This section will describe the two wave-based active control systems that have been used here to realise nonreciprocal sound transmission and absorption. Both control systems utilise the integration wave separation method proposed by

Table 1. The system parameters used to define the system setups shown in Fig. 1(a).

Duct diameter	D	x_1	x_2	x_3	x_4	Density (ρ_0)	Speed of sound (c_0)
0.1 m	0.02 m	-0.286 m	-0.243 m	0.243 m	0.286 m	1.21 kg/m ³	343 m/s

Zhu *et al.*¹⁶ to separate the positive and negative propagating waves in the upstream and downstream sections of the duct as shown in Fig. 1(a). Active control is then used to minimise either the transmitted or both the transmitted and reflected wave components to achieve broadband nonreciprocal sound transmission and absorption, respectively. In both proposed controllers, a feedforward filtered-reference least mean squares (FxLMS) algorithm has been used to adaptively calculate the optimal control signals that drive the control sources to minimise the transmitted and reflected waves. For conciseness, we focus here on the case where we attempt to impede the propagation of waves generated by the positive primary source and allow the free propagation of waves generated by the negative primary source. Therefore, the reference signal in both cases is the positive propagating incident wave, $A_+(n)$. If instead the objective was to reverse the direction of nonreciprocal behaviour, the negative propagating incident wave, $D_-(n)$, would instead be used as the reference signal, however, this scenario is left to inference here for conciseness. The block diagrams of the two proposed wave-based active controllers are shown in Fig. 2, with Fig. 2(a) showing the block diagram of the transmitted wave controller and Fig. 2(b) showing the absorption controller; the details of the two controllers are described in the following.

2.1.1 Nonreciprocal sound transmission controller

In the first instance, a transmitted wave controller can be used to drive a single monopole control source to minimise the positive propagating transmitted wave, $C_+(n)$, whilst allowing the transmitted wave propagating in the other direction, $B_-(n)$, to be unimpeded and to thus achieve nonreciprocal sound transmission. The error signal in this case is the positive propagating transmitted wave, $C_+(n)$, which can be written in terms of the control system responses as

$$e_T(n) = d_T(n) + \mathbf{R}_T(n)\mathbf{w}_T(n), \tag{1}$$

where

$$d_T(n) = \frac{d_3(n) + d_4(n)}{4} + \frac{c_0}{2\Delta x} \int_0^{T_s} d_3(n) - d_4(n) dt \tag{2}$$

is the transmitted wave due to the positive primary source, calculated using the wave separation method,¹⁶ Δx is the microphone spacing, and $d_3(n)$ and $d_4(n)$ are the pressures measured at the third and fourth pressure sensors due to the primary source;

$$\mathbf{w}_T(n) = [w_{T_0}, \dots, w_{T_{n-I}}]^T \tag{3}$$

is the vector of I FIR control filter coefficients;

$$\mathbf{R}_T(n) = [r_T(n), r_T(n-1), \dots, r_T(n-I+1)]^T \tag{4}$$

is the vector of filtered reference signals; and

$$r_T(n) = \frac{r_{3_2}(n) + r_{4_2}(n)}{4} + \frac{c_0}{2\Delta x} \int_0^{T_s} r_{3_2}(n) - r_{4_2}(n) dt \tag{5}$$

is the transmitted wave component corresponding to the filtered reference signals, which are given by

$$r_{t_2} = \sum_{j=0}^{J-1} g_{Tj} A_+(n-j), \tag{6}$$

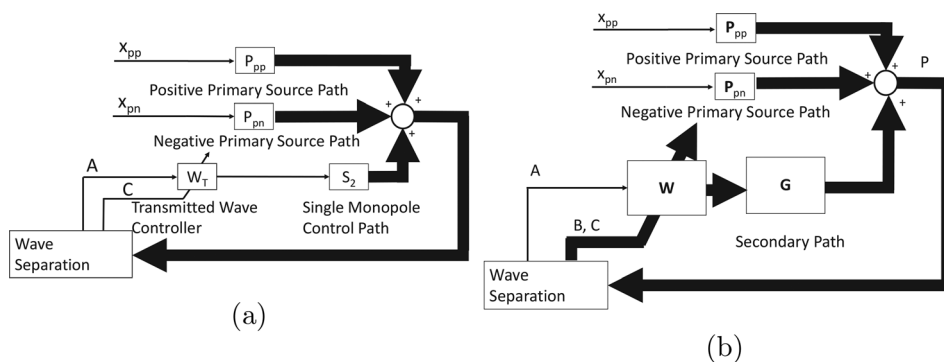


Fig. 2. The block diagram of the transmitted wave (a) and absorption (b) controllers used to achieve broadband nonreciprocal sound transmission and absorption. Thin lines relate to single channel signals, whilst thick lines relate to multichannel signals.

where A_+ is the reference signal and g_{ij} is the j th FIR filter coefficient of the J coefficient filter representing the plant response between the control source and the l th pressure sensor. The cost function in this case is the mean squared value of the error signal corresponding to the transmitted wave, which can be expressed as

$$J_T(n) = |e_T(n)|^2. \tag{7}$$

Substituting Eq. (1) into Eq. (7), gives the cost function in Hermitian quadratic form as

$$J_T(n) = \mathbf{w}_T^T(n) \mathbf{R}_T^T(n) \mathbf{R}_T(n) \mathbf{w}_T(n) + 2\mathbf{w}_T^T(n) \mathbf{R}_T^T(n) d_T(n) + |d_T(n)|^2 \tag{8}$$

Taking the derivative of the cost function with respect to the vector of FIR control filter coefficients, $\mathbf{w}_T(n)$, gives the gradient operator as

$$\frac{\partial J_T(n)}{\partial \mathbf{w}_T} = 2\mathbf{R}_T^T(n) e_T(n). \tag{9}$$

Following the method of steepest descent, the vector of FIR control filter coefficients can then be updated using an FxLMS algorithm, which can be expressed as

$$\mathbf{w}_T(n+1) = \mathbf{w}_T(n) - \mu \mathbf{R}_T^T(n) e_T(n), \tag{10}$$

where μ is a convergence gain, which controls the stability and speed of convergence. This algorithm will adapt the control filter coefficients to minimise the transmitted wave cost function given by Eq. (7).

2.1.2 Nonreciprocal sound absorption controller

The second control system considered here aims to achieve broadband nonreciprocal absorption control, which has not previously been demonstrated in the literature. The absorption controller uses a pair of monopole control sources to minimise the transmitted and reflected waves and thus maximise absorption. As above, we express the case here where we aim to absorb the incident wave generated by the positive primary source, whilst leaving the incident wave generated by the negative primary source unimpeded by control. The error signal in this case can be defined as

$$\mathbf{e}(n) = \mathbf{d}(n) + \mathbf{R}(n) \mathbf{w}(n), \tag{11}$$

where

$$\mathbf{d}(n) = [d_T(n), d_R(n)]^T \tag{12}$$

is the vector of disturbance signals consisting of the transmitted and reflected wave components due to the positive primary source, where $d_T(n)$ is given by Eq. (2) and

$$d_R(n) = \frac{d_1(n) + d_2(n)}{4} + \frac{c_0}{2\Delta x} \int_0^t d_1(n) - d_2(n) dt \tag{13}$$

is the reflected wave component due to the primary source and $d_1(n)$ and $d_2(n)$ are the pressures generated by the primary source at the first and second pressure sensors, respectively;

$$\mathbf{w}(n) = [w_{2_0}, w_{1_0}, \dots, w_{2_{n-I-1}}, w_{1_{n-I-1}}]^T \tag{14}$$

is the vector of FIR control filter coefficients, which in this case has dimensions of $2I \times 1$;

$$\mathbf{R}(n) = \begin{bmatrix} r_{T_2}(n), r_{T_1}(n), r_{T_2}(n-1), r_{T_1}(n-1), \dots, r_{T_2}(n-I+1), r_{T_1}(n-I+1) \\ r_{R_2}(n), r_{R_1}(n), r_{R_2}(n-1), r_{R_1}(n-1), \dots, r_{R_2}(n-I+1), r_{R_1}(n-I+1) \end{bmatrix}^T \tag{15}$$

is the matrix of filtered reference signals, where

$$r_{T_m} = \frac{r_{3_m}(n) + r_{4_m}(n)}{4} + \frac{c_0}{2\Delta x} \int_0^t r_{3_m}(n) - r_{4_m}(n) dt \tag{16}$$

and

$$r_{R_m} = \frac{r_{1_m}(n) + r_{2_m}(n)}{4} + \frac{c_0}{2\Delta x} \int_0^t r_{1_m}(n) - r_{2_m}(n) dt \tag{17}$$

are the transmitted and reflected wave components corresponding to the filtered reference signals, which are given by

$$r_{l_m} = \sum_{j=0}^{J-1} g_{lmj} A_+(n-j), \tag{18}$$

where g_{lmj} is the j th FIR filter coefficient of the J coefficient filter representing the plant responses from the m th control source to the l th pressure sensor. The cost function in this case is defined as the mean squared value of the sum of the transmitted and reflected wave components, which can be expressed as

$$J(n) = \mathbf{e}^T(n)\mathbf{e}(n). \tag{19}$$

Following the same procedure described in Sec. 2.1.1, the multichannel FxLMS algorithm in this case can be expressed as

$$\mathbf{w}(n+1) = \mathbf{w}(n) - \mu \mathbf{R}^T(n)\mathbf{e}(n). \tag{20}$$

3. Results

This section presents both the simulated and experimental performance of the proposed active controllers described in Sec. 2.1 with respect to both a positive and a negative propagating incident plane wave. In addition, the practical system and control sources used for the experimental validation are also described.

3.1 Simulation results

This section presents the results of a simulation-based study into the performance of the two control systems described in Sec. 2. For this theoretical study, the responses between the primary and control sources and the pressure sensors have been modelled assuming one-dimensional plane wave propagation in a duct. The primary source has been driven assuming a white noise excitation signal, band limited to frequencies between 560 and 1600 Hz, which define the limits of the proposed methodology for the considered geometry as discussed in Sec. 2. The performance of the two wave-based active controllers have been evaluated in terms of the transmitted, reflected and absorbed energy, normalised to the incident energy, when either a positive or negative propagating incident plane wave excites the system and the results of these simulations are shown in Figs. 3(a)–3(c). The experimental results are shown in Figs. 3(d)–3(f) and these results will be discussed further in Sec. 3.2. It should be reiterated that the controllers have been setup to control the positive incident wave, whilst allowing the negative incident wave to propagate unimpeded. Figure 3(a) shows the performance of the transmission controller (dashed magenta line) with respect to a positive propagating incident wave and Fig. 3(a) shows its behaviour with respect to a negative propagating incident wave (dashed black line). From Fig. 3(a) it can be seen that the transmission controller achieves zero transmission with respect to the positive propagating wave, whilst the transmission of the negative propagating wave is unaffected by the controller. Thus, demonstrating that this system achieves broadband nonreciprocal transmission control, however, it is insightful to also observe the behaviour of the system in terms of the reflection and absorption coefficients. In the case of the positive propagating incident wave, since the transmission controller does not constrain the upstream sound radiation from the control sources or consider the reflected energy, the active control system perfectly reflects the positive propagating incident wave and this can be seen from the unity reflection coefficient shown in Fig. 3(b); since the wave is perfectly reflected, there is no absorption in this case as shown in Fig. 3(c). When the incident sound field is propagating in the negative direction, it can be seen from the results presented in Figs. 3(b) and 3(c) that since the wave is perfectly transmitted, there is no reflection or absorption of the incident energy, therefore, as desired, the wave propagates as if there is no controller in place in this direction.

Extending the wave-based active control concept, an absorption controller has been described in Sec. 2.1.2, which aims to achieve nonreciprocal absorption behaviour. The proposed absorption controller has been implemented to absorb a positive propagating incident wave whilst allowing a negative propagating incident wave to pass unimpeded. The performance of this controller is shown in Figs. 3(a)–3(c) in terms of the three performance metrics when the system is excited by either a positive (solid magenta lines) or a negative (solid black lines) propagating incident wave respectively. From Fig. 3(c) it can be seen that the positive incident wave is perfectly absorbed across the presented bandwidth and thus the transmitted and reflected energy are both zero as shown in Figs. 3(a) and 3(b). Conversely, it can be seen from the results presented in Fig. 3(a) that the negative incident wave is perfectly transmitted. These results thus demonstrate that the proposed controller achieves broadband nonreciprocal absorption.

3.2 Experimental validation

The theoretical results presented in Sec. 3.1 have demonstrated that the proposed transmission and absorption active control strategies have the ability to achieve broadband nonreciprocal sound transmission and absorption, respectively. However, it is important to experimentally validate these results, since the performance of a practical system may be influenced by additional effects that are neglected in the theoretical model, such as imperfect anechoic terminations and finite-sized control loudspeakers. Thus, it is important to experimentally validate the simulation results shown in Fig. 3 and this has been carried out using the practical duct system shown in Fig. 1(b). The proposed active controllers described in Sec. 2.1 have been practically realised using a dSpace rapid prototyping DSP system. The practical system also uses antialiasing and reconstruction lowpass filters and amplifiers for both the primary and control sources. As in Sec. 3.1, the primary sources in the practical system are driven with band limited white noise, with a passband of 560–1600 Hz. Figure 1(b) shows a photograph of the experimental setup and Fig. 1(c) shows how both of the control sources have been practically

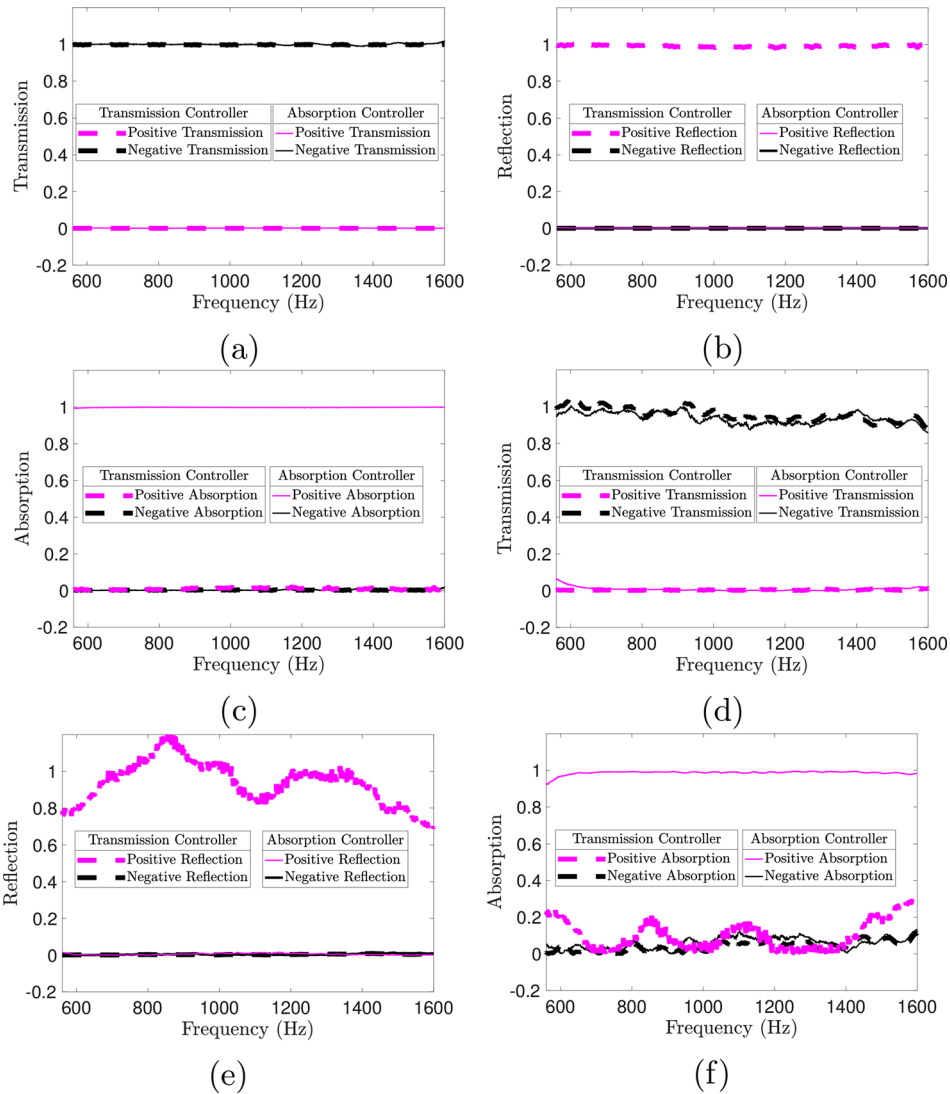


Fig. 3. The simulated (a)–(c) and experimental (d)–(f) performance of the transmission controller (dashed lines) and absorption controller (solid lines) in terms of the magnitude of the normalised transmitted (a),(d), reflected (b),(e) and absorbed (c),(f) energy for a positive propagating incident wave (magenta lines) and for a negative propagating incident wave (black lines).

realised using a pair of KDMG20008 loudspeakers mounted in closed back enclosures. The downstream facing loudspeaker, which is labelled q_{s1} in Fig. 1(c), is driven to minimise the transmitted wave via the transmitted wave controller and both of the loudspeakers shown in Fig. 1(c) are driven to maximise the sound absorption using the proposed absorption controller.

The results from the experimental implementation of the two nonreciprocal wave-based active control strategies are shown in Fig. 3 in terms of the transmission, reflection, and absorption performance metrics. The experimental results shown in Fig. 3 are largely consistent with the simulation results shown in Figs. 3(a)–3(c), confirming that the transmission and absorption controllers can drive the respective control sources to achieve broadband nonreciprocal sound transmission and absorption, respectively. In the case of the transmission controller, it is worth noting that for the positive incident wave case shown in Figs. 3(e) and 3(f), the absorption coefficient becomes negative at certain frequencies and the reflection coefficient is greater than unity, which means that the control strategy enhances the energy in the upstream section of the system at some frequencies, but still maintains zero transmission of the positive propagating incident wave. The differences between the simulation and experimental results for this controller are thought to be a result of the scattering from the physical, finite-sized control source located in the duct, which is not included in the theoretical model. In the case of the corresponding positive incident propagating wave results for the absorption controller, as shown in Figs. 3(e) and 3(f), this difference in performance does not occur since the controller in this case also attempts to minimise the reflection from the system and so inherently removes any scattering from the finite-sized control sources. Nevertheless, as

can be seen from the results presented in Fig. 3(d), both the transmission (dashed lines) and absorption (solid lines) controllers allow a negative propagating incident wave to pass largely unimpeded. There are some small variations over frequency in both cases, which are due to the terminations of the experimental duct not being perfectly anechoic, however, it is clear that both controllers realise broadband nonreciprocal behaviour.

4. Conclusions

The work presented in this paper has proposed and demonstrated two wave-based active control systems that can manipulate the transmitted and reflected waves independently to achieve broadband nonreciprocal sound transmission or absorption in a one-dimensional environment. The broadband nonreciprocal behaviour of both the transmission and absorption controllers has been demonstrated through theoretical simulations and an experimental implementation using a practical duct system. The low frequency limit is imposed by the assumption that the sensors used in the wave separation method are located in the far field of the control sources and the upper frequency limit is imposed by the assumption of plane wave propagation within the duct; nevertheless, nonreciprocal behaviour is demonstrated without introducing signal distortions over a bandwidth in excess of one octave. Furthermore, it has been highlighted that the proposed wave-based active control systems are fully adaptable, such that the direction of the broadband nonreciprocal behaviour can be reversed simply by changing the reference and error signals used by the wave-based active controllers.

The work presented in this paper shows the performance of one active unit cell, however, this concept could be extended to create an active acoustic metasurface consisting of an array of these active unit cells in order to achieve broadband nonreciprocal sound transmission or absorption in a two- or three-dimensional space.

Acknowledgments

This research was partially supported by an EPSRC iCASE studentship (Voucher number: 17000146) and the Intelligent Structures for Low Noise Environments EPSRC Prosperity Partnership (EP/S03661X/1).

References and links

- ¹D. N. Zotkin, R. Duraiswami, R. Grassi, and N. A. Gumerov, "Fast head-related transfer function measurement via reciprocity," *J. Acoust. Soc. Am.* **120**(4), 2202–2215 (2006).
- ²B. S. Kim, G. J. Kim, and T. K. Lee, "The identification of Tyre induced vehicle interior noise," *Appl. Acoust.* **68**(1), 134–156 (2007).
- ³B. Liang, S. Guo, J. Tu, D. Zhang, and J. C. Cheng, "An acoustic rectifier," *Nat. Mater.* **9**(12), 989–992 (2010).
- ⁴B. I. Popa and S. A. Cummer, "Non-reciprocal and highly nonlinear active acoustic metamaterials," *Nat. Commun.* **5**, 3398 (2014).
- ⁵Z. M. Gu, J. Hu, B. Liang, X. Y. Zou, and J. C. Cheng, "Broadband non-reciprocal transmission of sound with invariant frequency," *Sci. Rep.* **6**(1), 19824 (2016).
- ⁶A. Baz, "Active nonreciprocal acoustic metamaterials using a switching controller," *J. Acoust. Soc. Am.* **143**(3), 1376–1384 (2018).
- ⁷A. Baz, "Active nonreciprocal metamaterial using an eigen-structure assignment control strategy," *J. Acoust. Soc. Am.* **147**(4), 2656–2669 (2020).
- ⁸R. Fleury, D. L. Sounas, C. F. Sieck, M. R. Haberman, and A. Alù, "Sound isolation and giant linear nonreciprocity in a compact acoustic circulator," *Science* **343**(6170), 516–519 (2014).
- ⁹R. Fleury, D. L. Sounas, and A. Alù, "Subwavelength ultrasonic circulator based on spatiotemporal modulation," *Phys. Rev. B* **91**(17), 174306 (2015).
- ¹⁰Y. Chen, X. Li, H. Nassar, A. N. Norris, C. Daraio, and G. Huang, "Nonreciprocal wave propagation in a continuum-based metamaterial with space-time modulated resonators," *Phys. Rev. Appl.* **11**(6), 064052 (2019).
- ¹¹C. Shen, J. Li, Z. Jia, Y. Xie, and S. A. Cummer, "Nonreciprocal acoustic transmission in cascaded resonators via spatiotemporal modulation," *Phys. Rev. B* **99**(13), 134306 (2019).
- ¹²A. Sasmal, N. Geib, B. I. Popa, and K. Grosh, "Broadband nonreciprocal linear acoustics through a non-local active metamaterial," *New J. Phys.* **22**(6), 063010 (2020).
- ¹³N. Geib, A. Sasmal, Z. Wang, Y. Zhai, B. I. Popa, and K. Grosh, "Broadband nonreciprocal linear acoustics through a non-local active metamaterial," *Phys. Rev. B* **103**(16), 165427 (2021).
- ¹⁴Y. T. Fang and Y. C. Zhang, "Perfect nonreciprocal absorption based on metamaterial slab," *Plasmonics* **13**(2), 661–667 (2018).
- ¹⁵Q. Y. Wang, S. Liu, D. Gui, and H. F. Zhang, "Nonreciprocal absorption characteristics of one-dimensional cylindrical magnetized plasma photonic crystals," *Phys. Scr.* **96**(6), 065501 (2021).
- ¹⁶H. Zhu, R. Rajamani, and K. A. Stelson, "Active control of acoustic reflection, absorption, and transmission using thin panel speakers," *J. Acoust. Soc. Am.* **113**(2), 852–870 (2003).
- ¹⁷S. J. Elliott, J. Cheer, L. Bhan, C. Shi, and W. S. Gan, "A wavenumber approach to analysing the active control of plane waves with arrays of secondary sources," *J. Sound Vib.* **419**, 405–419 (2018).
- ¹⁸K. Hook, J. Cheer, and S. Daley, "A parametric study of an acoustic black hole on a beam," *J. Acoust. Soc. Am.* **145**(6), 3488–3498 (2019).